AD

AD 614060

TR-1267

MEASUREMENT OF ELECTROSTATIC CHARGE ON AIRCRAFT

by

Philip Krupen

Elmer B. Rogers

30 December 1964

COPY 2 OF 3

HARD COPY $

MICROFICHE $

HARRY DIAMOND LABORATORIES

The findings in this report are not to be construed as an official Department of the Army position, unless so designated by other authorized documents.

Reproduction of this document in whole or in part is prohibited except with permission of Edgewood Laboratories. However, DDC is authorized to reproduce the document for United States Government purposes.

Destroy this report when it is no longer needed. Do not return it to the originator.

Availability Notice

Qualified requesters may obtain copies of this report from DDC. DDC release to Clearinghouse for Federal Scientific and Technical Information is authorized.

Best
Available
Copy

CONTENTS

PAGE NO.

ABSTRACT. 5

1. INTRODUCTION 5

2. TEST METHOD 5

3. TEST EQUIPMENT 7

4. TEST PROCEDURE 10

5. RESULTS. 10

6. CONCLUSION 13

7. REFERENCES 13

APPENDIX A. 16-22

APPENDIX B. 23-25

APPENDIX C. 26-29

DISTRIBUTION. 31-33

ILLUSTRATIONS

Figure 1. Schematic diagram of test arrangement. 6

Figure 2. Pilot's view of induction plate. 8

Figure 3. Field layout 9

Figure 4. Recordings of induced voltage. 11

Figure A1. Circuit. 17

Figure A2. Applied voltage. 17

Figure A3. Driving and transfer functions 22

Figure B1. Test arrangement for measurement of proportionality factor. 24

Figure C1. Photographs of airplane overhead 27

Figure C2. Geometry of the optical system 28

ABSTRACT

The electrostatic charge on airplanes was determined from measurements of the charge induced on a large screen while the airplanes flew over it. The airplane charge was computed from a transfer function that involved the relaxation time of the sensing circuit and the passage time of the airplane. Corrections for variation in the height and displacement of the airplanes were made from laboratory measurements on scale models of the field equipment. The average charge on a jet-propelled F-86 fighter was found to be -35.4×10^{-6} coulomb and on a B-26 bomber, -0.56×10^{-6} coulomb. The corresponding aircraft potentials are approximately -141,000 and -1200 v.

1. INTRODUCTION

It has long been known that aircraft in flight carry an electric charge. The effects of this charge are usually observed when it is so large as to be hazardous as when the Zeppelin Hindenburg burst into flame or so troublesome as when precipitation static interferes with aircraft communication (ref 1,2). Such phenomena occur when the static charge has built up to the level where a spark or corona occurs. The extent of charging when conditions are not conducive to such a large accumulation is not so easily recognized.

The present investigation was made to determine to what extent airplanes are charged in clear weather.

2. TEST METHOD

There are many possible methods for measuring the electrostatic charge on aircraft. The method used by Ross Gunn and his associates (ref 1), wherein electric field meters were installed at various points on the surface of an airplane, was not feasible in this investigation because of the required major modifications to the airplane. Flying an airplane through a Faraday cage or into a screen in order to measure the full charge by induction or by charge transfer was obviously not feasible. The method selected, a modification of the Faraday cage technique, consisted in flying the airplanes over a large plate which detected the charge by induction. The flights were therefore restricted to low altitudes.

The test equipment was arranged as shown schematically in figure 1. P represents the induction plate and E the earth. The net resistance and capacitance between P and E are represented by $R_1 + R_2$ and C_2, respectively. The electric charge on an airplane, A, flying overhead induces a charge on P. A voltage proportional to that on P is recorded by an oscillograph, B.

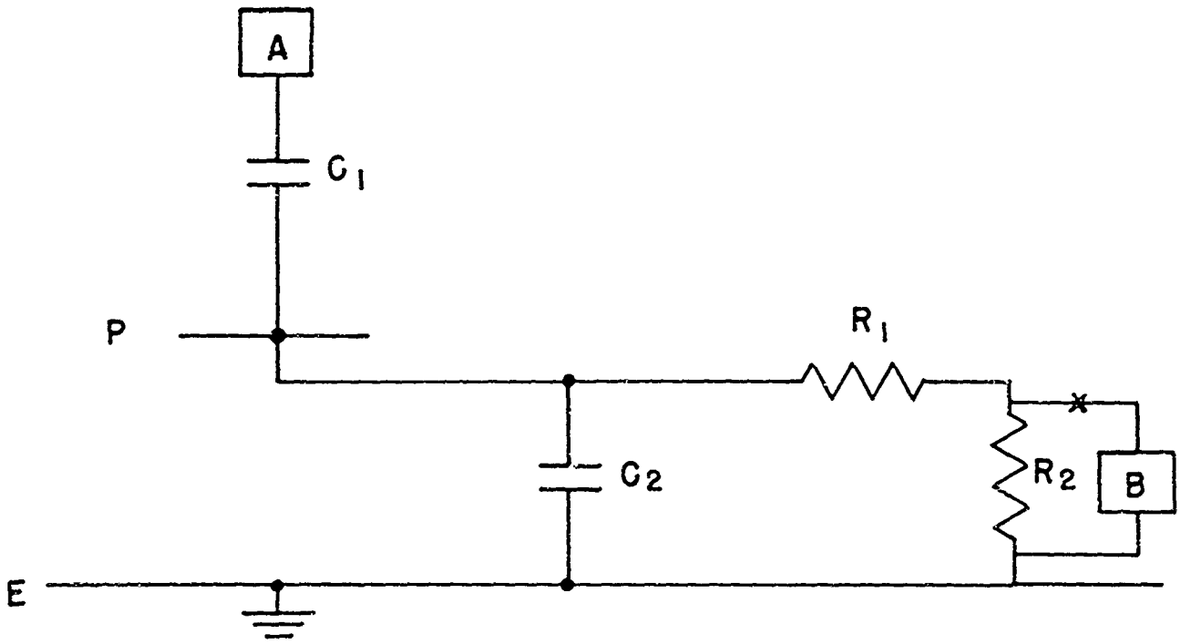

FIGURE 1. SCHEMATIC DIAGRAM OF TEST ARRANGEMENT

A relationship between the charge and the recorded signal is derived in appendix A. The equation used is

$$Q = \frac{2C_2 v_{max}}{k\ f(t)_{max}} \tag{1}$$

in which Q = charge on aircraft, coul

C_2 = capacitance between plate and ground, 0.0236 μf

k = proportionality factor

v = recorded signal, volts

$f(t)$ = transfer function

The determination of the proportionality factor, which represents the ratio of the peak induced charge on the plate to Q, is given in appendix B.

3. TEST EQUIPMENT

The detection equipment (fig. 2) was set up on an apron at Phillips Field, Aberdeen Proving Ground, Maryland. A metal ground screen consisting of 2-in. mesh netting, 150 by 150 ft, was spread out to establish a definite electrical ground. The induction plate consisted of 50 wood frames covered with 1-in. mesh wire netting and supported by 1-ft plastic legs. The frames were assembled over the center of the ground screen and connected together to form a plate 80 ft wide by 55 ft in the direction of the aircraft flight.

The recording equipment was located about 400 ft to the side of the detection equipment (fig. 3). A shielded cable connected the induction plate to the recorder. The capacitance of the plate and cable to ground (C_2, fig. 1) was measured and found to be 0.0236 μf. The resistance consisted of the recorder resistance (R_2, 10 meg) plus additional series resistance (R_1) needed for attenuation.

Auxiliary equipment was used to measure the velocity, height, and off-center displacement of an airplane each time it passed over the screen. Two photocell instruments were placed along the line of flight, 400 ft apart, one on each side of the screen. The aircraft speed was computed from the elapsed time between the two signals caused by obscuration. An open shutter movie camera was placed slightly beyond the second photocell to photograph the airplanes. The height and position of each airplane was determined accurately from the resulting photograph, as explained in appendix C. An alidade located to the side of the screens enabled a ground observer to give the pilot immediate information on the height of passage of the airplane.

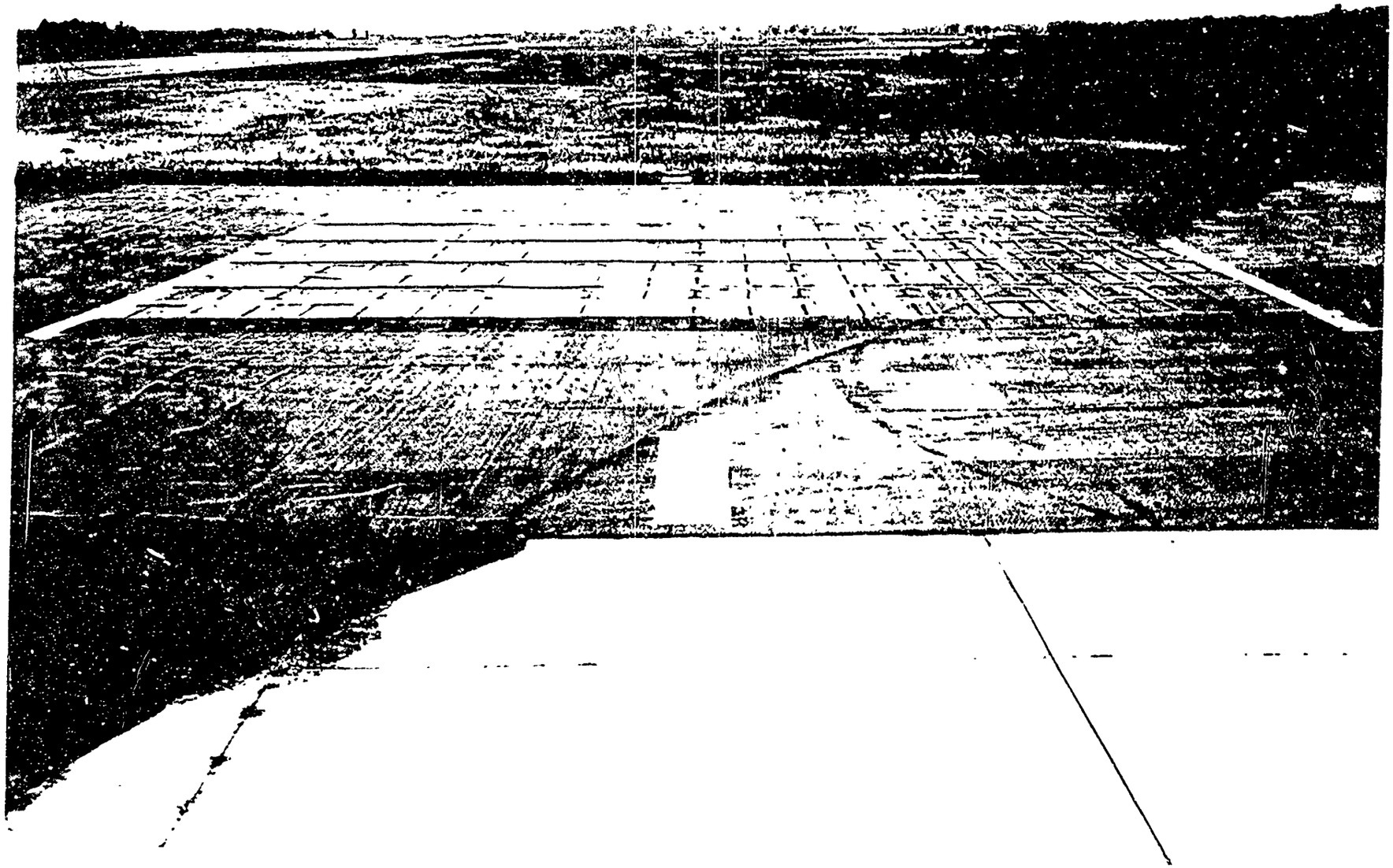

FIG. 2 PILOT'S VIEW OF INDUCTION PLATES

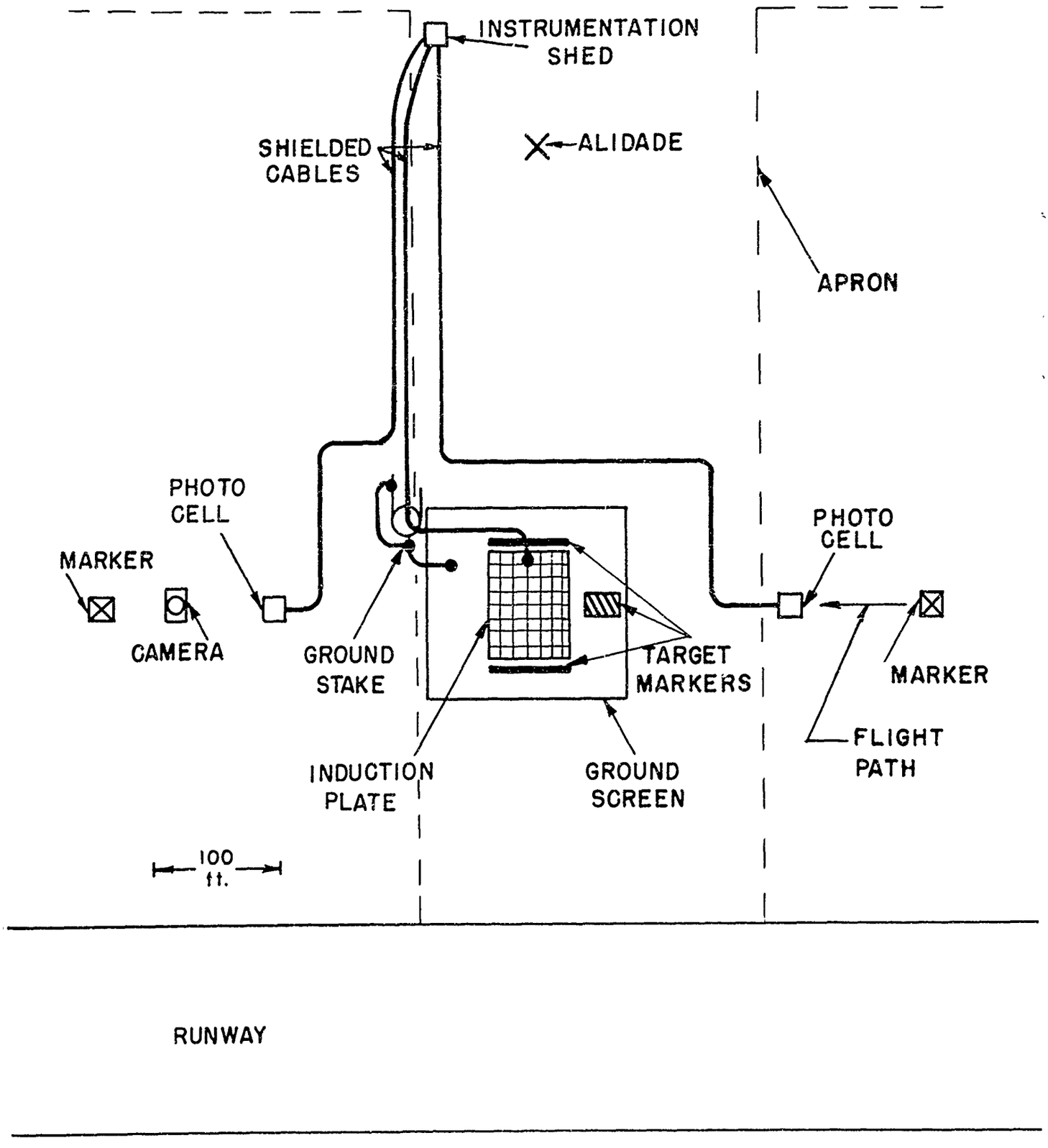

FIGURE 3. FIELD LAYOUT

4. TEST PROCEDURE

The electric charge was measured in clear weather on B-26 propeller-driven bombers flown by crews of the 6570th Test Group of the Air Force and on F-86 jet-propelled fighters flown by members of the Maryland Air National Guard. In addition, an L-19 observation plane and a C-54 cargo plane were invited to fly over the induction screen for observation while the apparatus was in place.

The pilots flew over the screen as low as safety limits permitted, levelling off about 4000 ft before the test area and, guided by ground markers and by the edge of the runway, tried to fly over the center of the screen. Heights over the screen ranged from 20 to 63 ft, and displacements from the center line ranged from zero to 25 ft. The velocities were usually close to their upper limits for the combat aircraft. Original plans to cover a range of velocities and other flight situations had to be abandoned because the permissible flying time of the aircraft was cut short.

Recordings of the induced voltages, such as those shown in figure 4, were obtained for each airplane passage. The upper trace (fig. 4A) is typical of those originally obtained for a B-26 with the test circuit shown in figure 1 with $R_1 = 0$. The very good agreement of this curve with the theoretical curve A in figure A3 confirms the derivation of the transfer function in appendix A. (Polarities are inverted.) Inasmuch as the only data desired for equation 1 were the peak values, a vacuum tube diode was later inserted in the circuit at point X (fig. 1) to eliminate the signal reversal and so establish a better base line. The resulting trace for a B-26 is shown in figure 4B and for an F-86 in figure 4C. These curves are for conditions comparable to those of curves B and C in figure A3.

5. RESULTS

The electrostatic charges on the airplanes were negative. The magnitudes were computed from equation 1 for those passages in which complete data were obtained. The heights and displacements were obtained in accordance with the procedure outlined in appendix C, and the k factor was obtained in accordance with the procedure outlined in appendix B. The peak value of the transfer function $f(t)_{max}$ was obtained from appendix A. The peak voltages (v_{max}) were read from the oscillograph traces. The results are tabulated for the F-86 and B-26 in tables 1 and 2, respectively.

The average electric charge found on the F-86 was -35.4×10^{-8} coul and on the B-26, -0.56×10^{-8} coul. The signals made by the passages of the C-54 and L-19 aircraft were similar to those shown in figure 4, and their average amplitudes were -5.8 and -4.6 v,

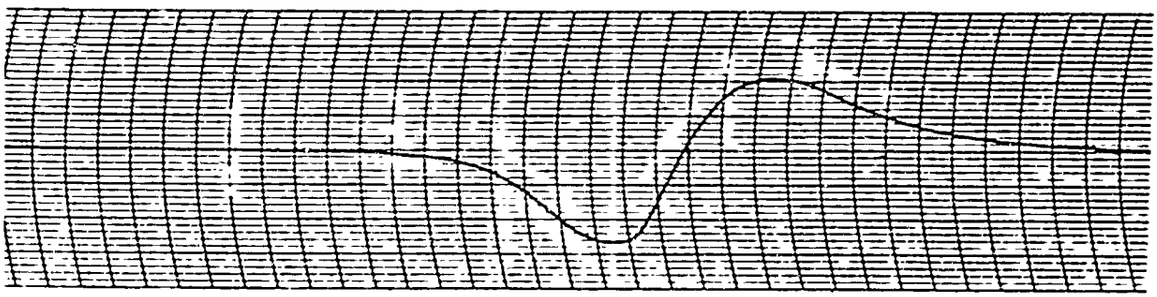

A. B-26 AIRPLANE, $R_1 = 0$

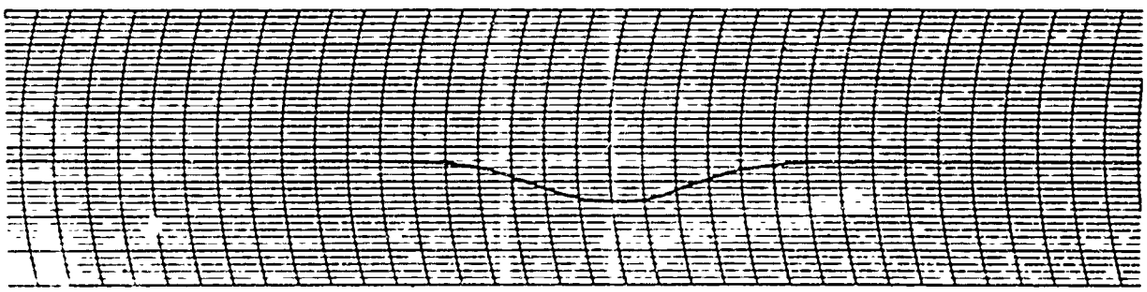

B. B-26 AIRPLANE, $R_1 = 100$ MEGOHMS

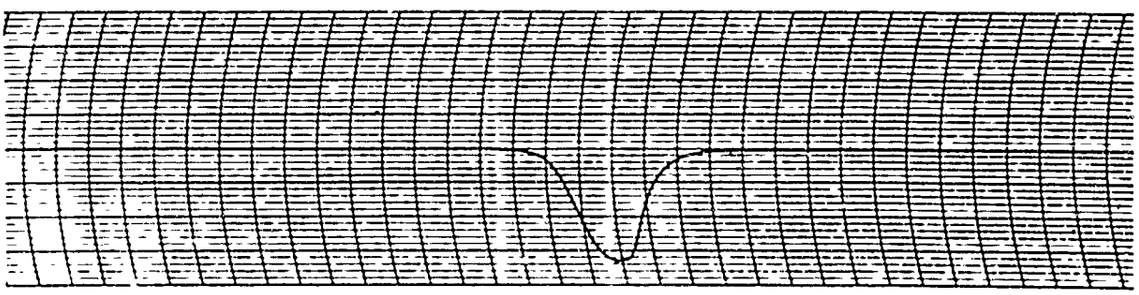

17701

C. F-86 AIRPLANE, $R_1 = 100$ MEGOHMS

FIG. 4 RECORDINGS OF INDUCED VOLTAGE

respectively. Although these signals exceeded those obtained with the B-26 bomber, the magnitudes of the associated airplane charge could not be evaluated because the auxiliary measurements for height and displacement were not recorded properly.

The potential of an airplane may be computed from its electric charge if its capacitance is known. Ross Gunn (ref 1) gave the capacitance of an airplane in esu as being approximately equal to 20 percent of its wing span in cm. In accordance with that criterion, the capacitance of the F-86 is

$$(20\%)\ (37.1\ \text{ft})\ (30.48\ \text{cm/ft})\ (1.11\ \text{pf/cm}) = 251\ \text{pf}$$

The average potential was therefore

$$(-35.4\times10^{-6}\ \text{coul})/(251\times10^{-12}\ \text{f}) = -141{,}000\ \text{v}.$$

The corresponding values for the B-26 are

$$(20\%)\ (70\ \text{ft})\ (30.48\ \text{cm/ft})\ (1.11\ \text{pf/cm}) = 473\ \text{pf}$$

and

$$(-0.56\times10^{-6}\ \text{coul})/(473\times10^{-12}\ \text{f}) = 1200\ \text{v}.$$

The magnitudes of the charge measured on the aircraft are shown in tables 1 and 2. Of 20 readings on the F-86, only one exceeded 52.4 μcoul, and only one was less than 26.1 μcoul. For the B-26, four readings exceeded 0.85 μcoul, five were less than 0.27 μcoul, and the remaining 16 were between those values. These distributions may be attributed to variation in the electrostatic charge on the aircraft from one run to another and from day to day, and to departure of the true values of k and $f(t)_{max}$ from the values used in the computations.

Most of the runs were made at maximum flight speeds. The number of flights at lower speeds was insufficient to determine any significant difference in the charging effects. Any possible effects may well have been hidden by other factors, such as the length of time flown at the lower speeds or passage through clouds before passage over the induction screen. No significant difference was found in the charge on the B-26 between runs with wicks and those without wicks. However, radio communications between the airplane and the ground were nearly severed with the wicks disconnected, which indicated that the airplane was losing charge in a very deleterious manner, perhaps from the antenna itself. The F-86 was not equipped with wicks; the jet exhaust probably served the purpose.

6. CONCLUSION

The electric charge on various military aircraft was measured in clear weather and at low altitudes by a method of charge induction without altering the construction or the usual flight procedures of the aircraft. The polarity of the charge was found to be negative. The average charge on the F-86 jet aircraft, 35.4 μcoul, was much greater than that on the B-26 propeller aircraft, 0.56 μcoul. These corresponded to potentials on the aircraft of about 141,000 and 1200 v, respectively. The magnitudes of the electric charge on L-19 and C-54 airplanes could not be computed although they were judged to be significant from the induced voltage measurements. It would be desirable to conduct further tests to study the accumulation of electric charge on aircraft under different conditions.

7. REFERENCES

(1) Ross Gunn, et al, Technical Reports, Army-Navy Precipitation Static Project, Proceedings of the IRE, Vol 34 (April 1946) pp 156-177, (May 1946) pp 234-254.

(2) T. Lyle Harlor, A. R. Jordan, and D. G. Murray, Development of Aircraft Discharge Methods, Final Report, Denver Research Institute Project No. 43, University of Denver, 15 April 1956.

(3) C. Ravitsky and R. G. Humphrey, Status of Infrared Fuzing, DOFL Report TR-429, December 1956 (C)

TABLE 1. RESULTS WITH F-86 AIRPLANES[a]

Velocity (mph)	Height (%WS)[b]	Displacement (%WS)[b]	Proportionality (k)	(R_1+R_2)[c] (meg)	Peak Signal[d] (v_{max}, v)	Charge on Airplane[d] (10^{-6} coul)
590	149	32	0.17	110	220	32.0
590	127	5	0.24	110	275	28.4
345	74	38	0.39	110	140	8.9
345	66	30	0.44	110	465	26.1
580	90	46	0.32	110	385	29.8
580	138	32	0.20	110	275	34.0
580	116	5	0.27	110	330	30.2
580	119	14	0.26	110	360	34.3
580	116	24	0.26	110	330	31.4
535	100	11	0.32	110	440	34.0
560	105	19	0.30	110	415	34.2
610	54	68	0.43	110	910	52.4
600	105	23	0.30	110	690	56.9
590	72	11	0.42	110	495	29.2
610	103	50	0.28	110	385	34.0
550	130	20	0.22	110	410	46.1
560	122	24	0.24	110	440	45.4
590	66	22	0.44	110	700	39.4
610	97	22	0.32	110	550	42.5
600	77	32	0.38	110	605	39.4
					Mean	35.4

Notes:

a. Diode in circuit for all runs.

b. The height of the lower fuselage surface above the induction screen and the displacement of the flight path from the center line of the plate are given in percentage of the wing span (WS). The wing span of the F-86 is 37.1 ft.

c. R_1+R_2 refers to the circuit of figure 1 and affects the transfer function, f(t). For these passages $f(t)_{max}$ is 1.908.

d. The polarity of the signal voltage and the charge is negative.

TABLE 2. RESULTS WITH B-26 AIRPLANES

Velocity (mph)	Height (%WS)[a]	Displacement (%WS)[a]	Proportionality (k)	(R_1+R_2)[b] (meg)	Peak Signal[c] (v_{max}, v)	Charge on Airplane[c] (10^{-6} coul)
330	50	28	0.145	10	0.95	0.50
330	90	50	0.065	10	1.65	2.00
320	68	45	0.090	10	1.05	0.85
370	65	26	0.110	10	0.75	0.52
340[d]	5[illegible]	11	0.145	10	3.0	1.59
330	57	9	0.110	10	2.6	1.81
320	66	14	0.110	10	1.8	1.28
340	68	19	0.105	10	0.6	0.41
340	44	32	0.165	10	0.2	0.09
210	32	13	0.245	110	3.3	0.38
215	42	6	0.195	110	0.6	0.09
210	41	14	0.195	110	3.6	0.51
260	59	7	0.130	110	1.4	0.30
260	34	14	0.230	110	2.2	0.27
315	36	19	0.215	110	0.8	0.11
330[e]	54	11	0.140	110	2.5	0.49
340	53	17	0.140	110	1.7	0.33
340	44	9	0.180	110	0.6	0.09
325	33	0	0.250	110	2.8	0.31
310	34	0	0.240	110	2.8	0.32
340	44	9	0.180	110	0.3	0.05
325	46	10	0.170	110	2.2	0.33
310	46	16	0.170	110	2.2	0.35
300	35	0	0.235	110	3.3	0.40
					Mean	0.56

Notes:

a. The height of the lower fuselage surface above the induction screen and the displacement of the flight path from the center line of the plate are given in percentage of the wing span (%WS). The wing span of the B-26 airplane is 70.0 ft.

b. $R_1 + R_2$ refers to the circuit of figure 1 and affects the transfer function, f(t). $f(t)_{max} = 0.616$ for $R_1 + R_2 = 10$ meg and $f(t)_{max} = 1.677$ for $R_1 + R_2 = 110$ meg for these passages.

c. The polarity of the signal voltage and the charge is negative.

d. Diode in circuit for this run and following runs.

e. Antistatic wicks disconnected for this run and following runs.

APPENDIX A—DERIVATION AND EVALUATION OF THE TRANSFER FUNCTION

The induction screen over which the airplane flies will be considered a solid plate, P, (fig. 1). A voltage pulse is recorded on the oscillograph, B, for each flyover. This pulse is the result of an electric charge q induced in the capacitor C_2 and the capacitance C_1. The maximum value of q is

$$q_{max} = kQ \tag{A1}$$

where Q is the charge on the airplane and $0 < k < 1$. This proportionality factor, k, may be obtained from scale model measurements, as described in appendix B.

During the flyover, the charge q depends on an assumed driving voltage v_o (fig. A1, derived from fig. 1) so that

$$q = \frac{C_1 C_2}{C_1 + C_2} v_o \tag{A2}$$

if R is infinitely large. Also,

$$q = C_2 v \tag{A3}$$

If no charge were lost from C_2 during the flyover, q_{max} could be computed simply from v_{max} read on the oscillograph tape. However, since charge is lost through R, a functional relationship between q and v must be derived.

The characteristics of the voltage v_o are that it is initially zero, reaches a maximum when the airplane is directly over the screen, and returns symmetrically to zero afterward, as indicated in figure A2, It may be considered as one cycle of the sinusoidal wave given by

$$v_o = \begin{cases} \frac{V_o}{2}\left(1 - \cos\frac{2\pi t}{T}\right), & 0 < t < T \\ 0, & t < 0,\ t > T \end{cases} \tag{A4}$$

where V_o = undetermined maximum value of v_o

t = elapsed time

T = period during which the charge on the airplane is effective.

From figure A1

$$v_o = \frac{1}{C_1}\int_{-\infty}^{t} i_o d\tau + v \tag{A5}$$

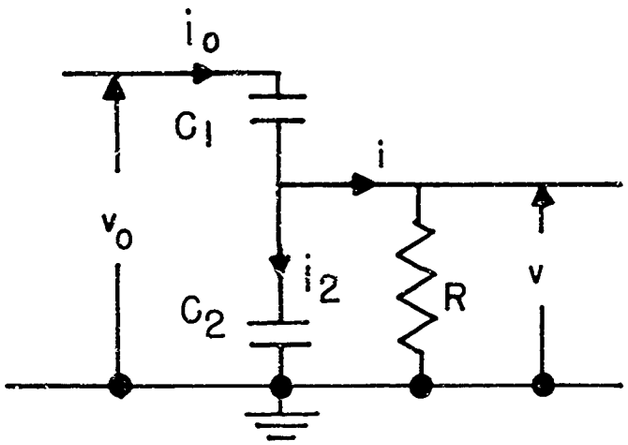

FIGURE A1. CIRCUIT

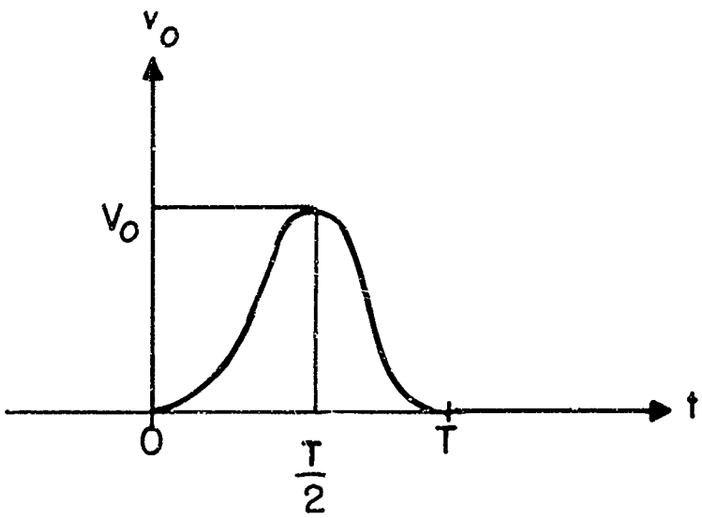

FIGURE A2. APPLIED VOLTAGE

$$v = \frac{1}{C_2} \int_{-\infty}^{t} i_2 \, d\tau = iR \tag{A6}$$

$$i_o = i + i_2 \tag{A7}$$

From equations A4, A5, and A6

$$\frac{1}{C_1} \int_{-\infty}^{t} i_o d\tau + iR = \begin{cases} 0, \ t < 0 \\ \frac{V_o}{2} \left(1 - \cos \frac{2\pi t}{T}\right), \ 0 < t < T \\ \frac{V_o}{2} \left(1 - \cos \frac{2\pi t}{T}\right) - \frac{V_o}{2} \left[1 - \cos \frac{2\pi (t-T)}{T}\right], \ t > T \end{cases} \tag{A8}$$

Since $v_o = v = i_o = i = i_2 = 0$ for $t < 0$, the application of Laplace transforms yields

$$\frac{\bar{i}_o}{C_1 s} + R\,\bar{i} = \begin{cases} \frac{V_o}{2s} \left(\frac{\beta^2}{s^2 + \beta^2}\right), \ 0 < t < T \\ \frac{V_o}{2s} \left(\frac{\beta^2}{s^2 + \beta^2}\right) \left(1 - e^{-Ts}\right), \ t > T \end{cases} \tag{A9}$$

in which

$$\beta = \frac{2\pi}{T} \tag{A10}$$

From equations A6 and A7,

$$\bar{i}_o = \bar{i} + \bar{i}_2$$

$$= \bar{i}(1 + RC_2 s) \tag{A11}$$

Substituting equation A11 into A9 and clearing of fractions

$$\left[1 + R(C_1 + C_2)s\right] \bar{i} = \begin{cases} \frac{V_o C_1 \beta^2}{2} \left(\frac{1}{s^2 + \beta^2}\right), \ 0 < t < T \\ \frac{V_o C_1 \beta^2}{2} \left(\frac{1 - e^{-Ts}}{s^2 + \beta^2}\right), \ t > T. \end{cases} \tag{A12}$$

In the interval $0<t<T$

$$\bar{i} = \frac{V_o C_1 \beta^2 \gamma}{2} \left(\frac{1}{s^2 + \beta^2}\right) \left(\frac{1}{s + \gamma}\right) \tag{A13}$$

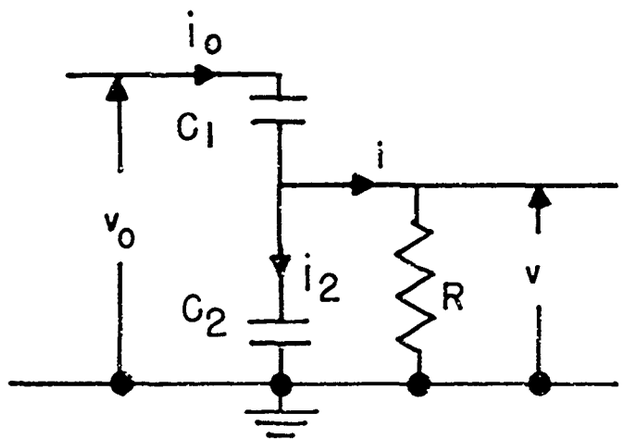

FIGURE A1. CIRCUIT

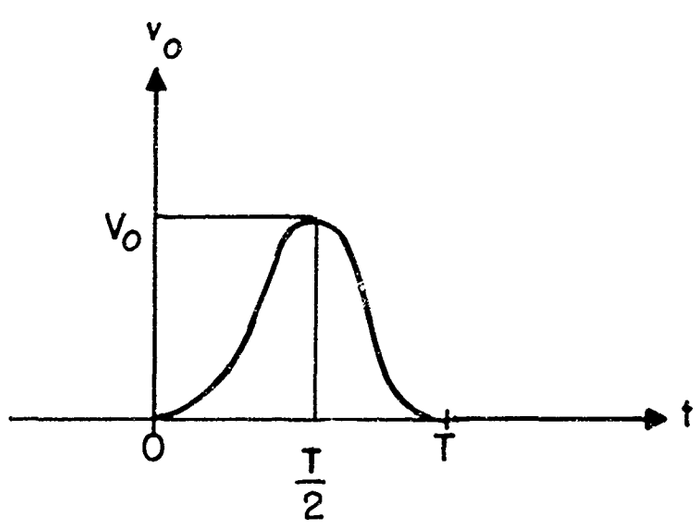

FIGURE A2. APPLIED VOLTAGE

$$v = \frac{1}{C_2} \int_{-\infty}^{t} i_2 \, d\tau = iR \tag{A6}$$

$$i_o = i + i_2 \tag{A7}$$

From equations A4, A5, and A6

$$\frac{1}{C_1} \int_{-\infty}^{t} i_o d\tau + iR = \begin{cases} 0, \ t < 0 \\ \frac{V_o}{2} \left(1 - \cos \frac{2\pi t}{T}\right), \ 0 < t < T \\ \frac{V_o}{2} \left(1 - \cos \frac{2\pi t}{T}\right) - \frac{V_o}{2} \left[1 - \cos \frac{2\pi (t-T)}{T}\right], \ t > T \end{cases} \tag{A8}$$

Since $v_o = v = i_o = i = i_2 = 0$ for $t < 0$, the application of Laplace transforms yields

$$\frac{\bar{i}_o}{C_1 s} + R\,\bar{i} = \begin{cases} \frac{V_o}{2s} \left(\frac{\beta^2}{s^2 + \beta^2}\right), \ 0 < t < T \\ \frac{V_o}{2s} \left(\frac{\beta^2}{s^2 + \beta^2}\right) \left(1 - e^{-Ts}\right), \ t > T \end{cases} \tag{A9}$$

in which

$$\beta = \frac{2\pi}{T} \tag{A10}$$

From equations A6 and A7,

$$\bar{i}_o = \bar{i} + \bar{i}_2$$

$$= \bar{i}(1 + RC_2 s) \tag{A11}$$

Substituting equation A11 into A9 and clearing of fractions

$$\left[1 + R(C_1 + C_2)s\right] \bar{i} = \begin{cases} \frac{V_o C_1 \beta^2}{2} \left(\frac{1}{s^2 + \beta^2}\right), \ 0 < t < T \\ \frac{V_o C_1 \beta^2}{2} \left(\frac{1 - e^{-Ts}}{s^2 + \beta^2}\right), \ t > T. \end{cases} \tag{A12}$$

In the interval $0 < t < T$

$$\bar{i} = \frac{V_o C_1 \beta^2 \gamma}{2} \left(\frac{1}{s^2 + \beta^2}\right) \left(\frac{1}{s + \gamma}\right) \tag{A13}$$

in which

$$\gamma = \frac{1}{R(C_1 + C_2)} \tag{A14}$$

On taking the inverse Laplace transform

$$i = \left[\frac{V_o C_1 \beta^2 \gamma}{2} \quad \frac{e^{-\gamma t}}{\beta^2 + \gamma^2} + \frac{\sin(\beta t - \psi)}{\beta(\beta^2 + \gamma^2)^{\frac{1}{2}}}\right] \tag{A15}$$

in which

$$\psi = \tan^{-1} \frac{\beta}{\gamma} \tag{A16}$$

In the interval t> T

$$\bar{i} = \frac{V_o C_1 \beta^2 \gamma}{2} \quad \left[\frac{1 - e^{-Ts}}{(s^2 + \beta^2)\ (s + \gamma)}\right] \tag{A17}$$

The inverse transform is

$$i = \frac{V_o C_1 \beta^2\ \gamma}{2} \left(\frac{\beta^2}{\beta^2 + \gamma^2}\right) (1 - e^{\gamma T})\ e^{-\gamma t} \tag{A18}$$

Multiplying equations A15 or A18 (according to whether t<T or t>T) by R gives the measured signal v. Rearranging terms gives

$$v = \frac{V_c}{2} \quad \frac{C_1}{C_1 + C_2}\ f(t) \tag{A19}$$

where

$$f(t) = \begin{cases} \dfrac{\beta^2}{\beta^2 + \gamma^2} \left[e^{-\gamma t} + \left(\dfrac{\beta^2 + \gamma^2}{\beta^2}\right)^{\frac{1}{2}} \sin(\beta t - \psi)\right], & 0<t<T \\ \dfrac{\beta^2}{\beta^2 + \gamma^2} \left[(1 - e^{\gamma T})\ e^{-\gamma t}\right], & t>T \end{cases} \tag{A20}$$

Equation A19 includes the undetermined constant V_o and the unknown capacitance C_1, both of which can be eliminated. From equation A2

$$q_{max} = \frac{C_1 \; C_2}{C_1 + C_2} \; Vo \tag{A21}$$

Substituting Vo from this equation into Equation A19

$$v = \frac{q_{max} \; f(t)}{2C_2} \tag{A22}$$

Substituting from equation A1

$$v = \frac{kQ \; f(t)}{2C_2} \tag{A23}$$

from which

$$Q = \frac{2C_2 \; v}{k \; f(t)} \tag{A24}$$

Since v and f(t) attain their maximum values simultaneously

$$Q = \frac{2C_2 v_{max}}{k \; f(t)_{max}} \tag{1}$$

This is the formula given in the text for the computation of Q. It can be seen that it has the form of $C_2 v$ multiplied by correction terms.

Values of the transfer function were computed not only at its maximum but over a large interval of time in order to check its validity. The parameters, defined above are

$$\beta = \frac{2\pi}{T} \tag{A10}$$

$$\gamma = \frac{1}{R(C_1 + C_2)} \tag{A14}$$

$$\psi = \tan^{-1} \frac{\beta}{\gamma} \tag{A16}$$

$$T = \text{effective flyover interval} \tag{A4}$$

R = 10 meg for some flights and 110 meg for others. C_2 was measured and found to be 0.0236 μf. C_1 was not measured, but it is very much smaller than C_2. The capacitance of the B-26 bomber to all

in which

$$\gamma = \frac{1}{R(C_1 + C_2)} \tag{A14}$$

On taking the inverse Laplace transform

$$i = \left[\frac{V_o C_1 \beta^2 \gamma}{2} \quad \frac{e^{-\gamma t}}{\beta^2 + \gamma^2} + \frac{\sin(\beta t - \psi)}{\beta(\beta^2 + \gamma^2)^{\frac{1}{2}}}\right] \tag{A15}$$

in which

$$\psi = \tan^{-1} \frac{\beta}{\gamma} \tag{A16}$$

In the interval t> T

$$\bar{i} = \frac{V_o C_1 \beta^2 \gamma}{2} \quad \left[\frac{1 - e^{-Ts}}{(s^2 + \beta^2)\ (s + \gamma)}\right] \tag{A17}$$

The inverse transform is

$$i = \frac{V_o C_1 \beta^2\ \gamma}{2} \left(\frac{\beta^2}{\beta^2 + \gamma^2}\right) (1 - e^{\gamma T})\ e^{-\gamma t} \tag{A18}$$

Multiplying equations A15 or A18 (according to whether t<T or t>T) by R gives the measured signal v. Rearranging terms gives

$$v = \frac{V_c}{2} \quad \frac{C_1}{C_1 + C_2} \ f(t) \tag{A19}$$

where

$$f(t) = \begin{cases} \dfrac{\beta^2}{\beta^2 + \gamma^2} \left[e^{-\gamma t} + \left(\dfrac{\beta^2 + \gamma^2}{\beta^2}\right)^{\frac{1}{2}} \sin(\beta t - \psi)\right], & 0<t<T \\ \dfrac{\beta^2}{\beta^2 + \gamma^2} \left[(1 - e^{\gamma T})\ e^{-\gamma t}\right], & t>T \end{cases} \tag{A20}$$

Equation A19 includes the undetermined constant V_o and the unknown capacitance C_1, both of which can be eliminated. From equation A2

$$q_{max} = \frac{C_1 \; C_2}{C_1 + C_2} \; Vo \tag{A21}$$

Substituting Vo from this equation into Equation A19

$$v = \frac{q_{max} \; f(t)}{2C_2} \tag{A22}$$

Substituting from equation A1

$$v = \frac{kQ \; f(t)}{2C_2} \tag{A23}$$

from which

$$Q = \frac{2C_2 \; v}{k \; f(t)} \tag{A24}$$

Since v and f(t) attain their maximum values simultaneously

$$Q = \frac{2C_2 v_{max}}{k \; f(t)_{max}} \tag{1}$$

This is the formula given in the text for the computation of Q. It can be seen that it has the form of $C_2 v$ multiplied by correction terms.

Values of the transfer function were computed not only at its maximum but over a large interval of time in order to check its validity. The parameters, defined above are

$$\beta = \frac{2\pi}{T} \tag{A10}$$

$$\gamma = \frac{1}{R(C_1 + C_2)} \tag{A14}$$

$$\psi = \tan^{-1} \frac{\beta}{\gamma} \tag{A16}$$

$$T = \text{effective flyover interval} \tag{A4}$$

R = 10 meg for some flights and 110 meg for others. C_2 was measured and found to be 0.0236 μf. C_1 was not measured, but it is very much smaller than C_2. The capacitance of the B-26 bomber to all

space was computed to be 475 pf and its parallel plate capacitance to the induction plate when directly over it was computed to be 82 pf. The values for the F-86 fighter are smaller, 250 pf and 32 pf. respectively. Hence, C_1+C_2 was taken as 0.0237 μf for the bomber and 0.0236 μf for the fighter. T was taken as 2 sec for the bomber, which corresponds to 440 ft on either side of the induction plate at a speed of 300 mph. T was taken as 1/2 sec for the smaller jet fighter, which corresponds to 220 ft on either side of the induction plate at a speed of 600 mph.

The results of the computations are shown graphically in figure A3. The similarity of curve A of figure A3 with the upper trace of figure 4 is apparent. Likewise, the curve C of figure A3 is similar to the lower trace of figure 4, although a discharge diode was present in the field test circuit. It can be noted that the area under the positive portion of each computed curve equals the area under the negative portion, which is to be expected inasmuch as the induction plate returns to zero potential after the airplane departs.

The maximum possible value of f(t) occurs when $R=\infty$ which makes $\gamma=0$, $f(t)=1 - \cos \beta t$, an $f(t)_{max}=2$. f(t) then becomes the same as the driving function, v_o (fig. A3) and equation 1 reduces to the ideal case

$$Q = \frac{C_2 v_{max}}{k} \tag{A25}$$

The following maximum values of f(t), used in the computations for Q, were calculated from equations A10, A14, A16, and A20.

Aircraft	R(meg)	T(sec)	$f(t)_{max}$
B-26	10	2	0.616
B-26	110	2	1.677
F-86	110	1/2	1.908
-	∞	-	2.000

It can be seen that the theoretical limit value of f(t) is almost reached with R = 110 megohms, especially in the tests with the F-86 jet airplane.

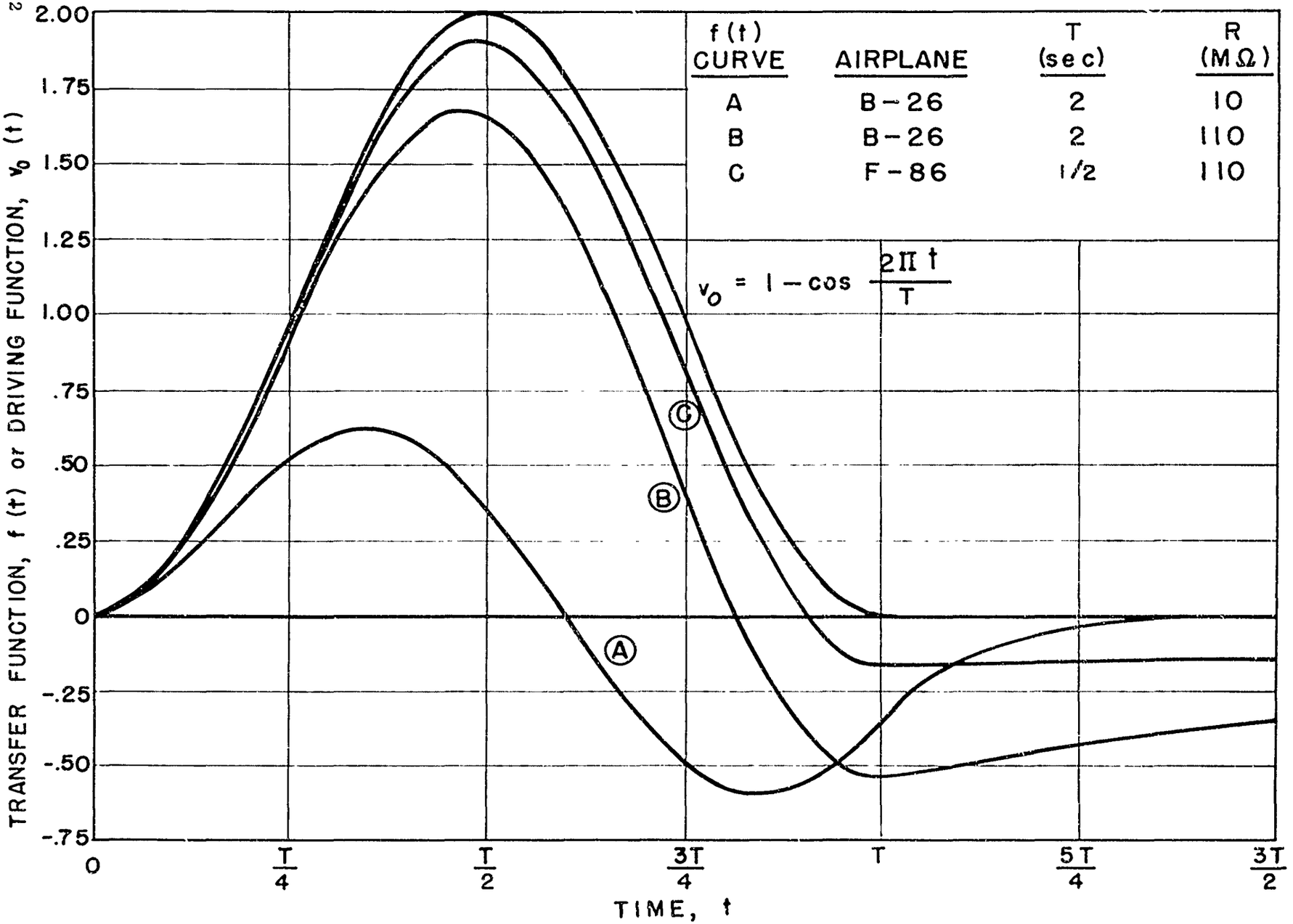

FIGURE A3. DRIVING AND TRANSFER FUNCTIONS

APPENDIX B—DETERMINATION OF THE PROPORTIONALITY FACTOR k

The proportionality factor k is the largest fraction of the total aircraft charge, Q, which is induced on the induction plate for a given flight path of the aircraft. Thus, if q is the charge on the plate

$$k = \frac{q_{max}}{Q} \tag{B1}$$

The proportionality factor was therefore determined for those positions for which the airplane is at the point of closest approach to the induction plate for a given flight path, so that q is maximum.

Values of k were measured in the laboratory on scale models of the equipment used in the field. A model of the B-26 airplane having scale factor of 67:1 was assembled and coated with silver paint. (The wing span of a B-26 is 70 ft; that of the model was 12 1/2 in.) An induction plate and a ground screen were built to the same scale and placed in the proper positions, as shown in figure B1. The model was suspended above the screen so that its belly could be placed at known heights and at known displacements off the center line. (The ruler in the photograph was not present during test measurements.) A similar mockup was made for the F-86 model, which had a scale of 48:1. (The wing span of an F-86 is 35.1 ft; that of the model 9.25 in.)

The ground screen was connected electrically to earth. An electrostatic voltmeter was connected between the ground screen and the induction plate to measure the electric charge induced on the plate. The capacitance of the induction plate configuration was measured over the complete deflection range of the voltmeter so that the charge could be calculated from the voltage reading.

A measurement of the proportionality factor was started with the induction plate at zero potential and the airplane at a distance of more than 5 ft from the screens. The airplane was charged to a potential of approximately 5000 v and brought to a predetermined position over the screens. The associated electrostatic voltmeter reading was noted, from which the corresponding value of induced charge was later computed from the formula Q = CV. The full charge on the airplane was then measured by bringing it into contact with the induction plate. The ratio of the two charge measurements yielded the proportionality factor k.

The values of k determined in this way for different combinations of height and displacement are listed in tables B1 and B2, in which the position coordinates are given in terms of airplane wing spans. This table was used in the computations of the charge on both the F-86 and the B-26 aircraft. Interpolation between tabulated values was done graphically.

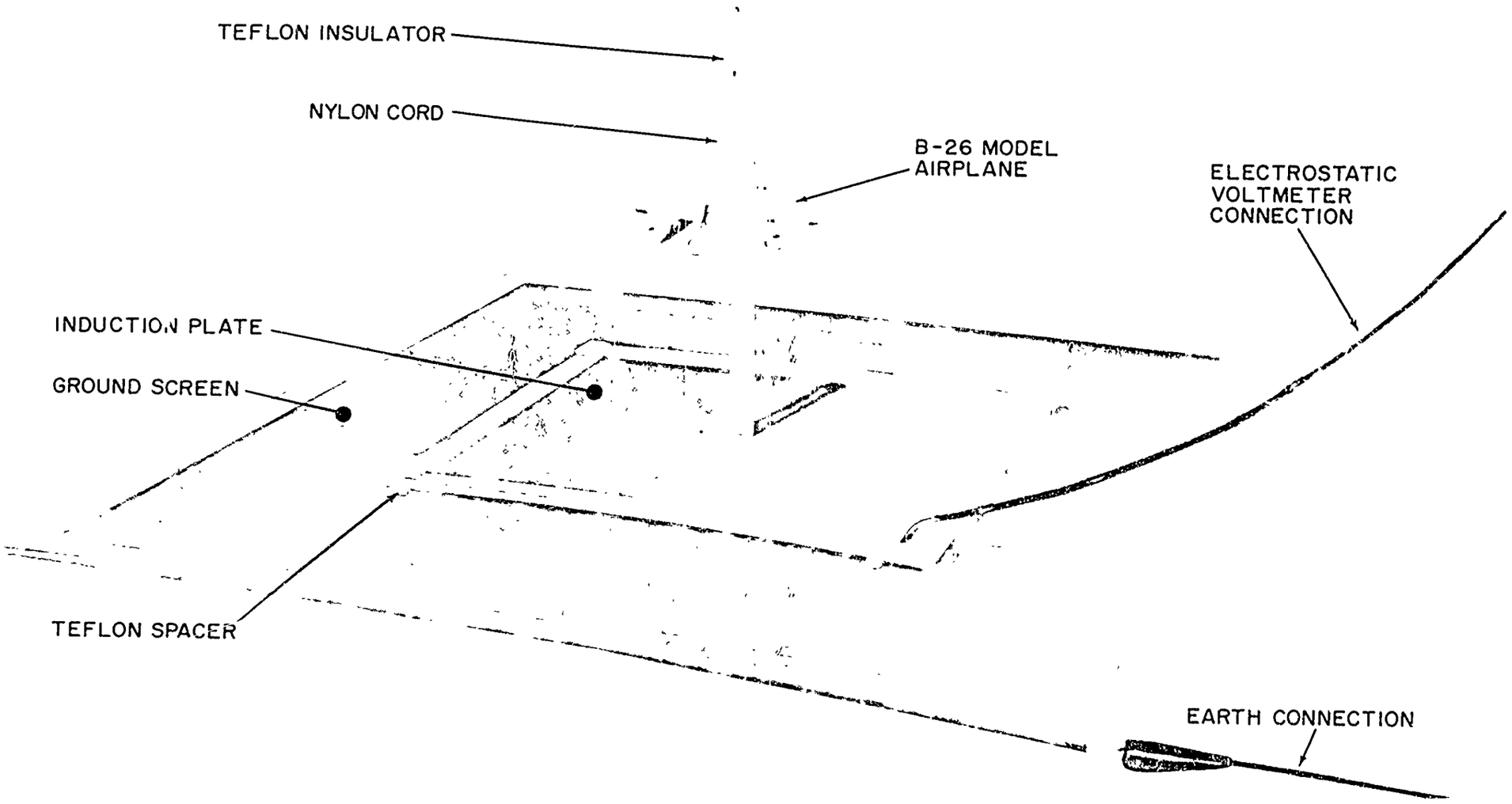

FIGURE BI. TEST ARRANGEMENT FOR MEASUREMENT OF PROPORTIONALITY FACTOR.

TABLE B1. PROPORTIONALITY FACTOR, k, FOR DIFFERENT POSITIONS OF THE F86 AIRCRAFT

Height*	Displacement from Center Line*				
	0.00	0.25	0.50	0.75	1.00
0.00	1.000	1.000	1.000	1.000	1.000
0.25	0.685	0.703	0.678	0.593	0.461
0.50	0.554	0.519	0.490	0.404	0.357
0.75	0.400	0.403	0.352	0.320	0.269
1.00	0.321	0.310	0.294	0.269	0.224
1.25	0.250	0.250	0.218	0.187	0.177
1.50	0.191	0.175	0.152	0.124	0.133
2.00	0.111	0.099	0.109	0.072	0.073

TABLE B2. PROPORTIONALITY FACTOR, k, FOR DIFFERENT POSITIONS OF THE B26 AIRCRAFT

Height*	Displacement from Center Line*			
	0.00	0.25	0.50	0.75
0.00	1.000	1.000	1.000	1.000
0.25	0.317	0.314	0.267	0.116
0.50	0.161	0.152	0.116	0.076
0.75	0.098	0.087	0.082	0.052
1.00	0.066	0.077	0.056	0.038

*Expressed as fractions of a wing span.

APPENDIX C—DETERMINATION OF POSITION OF AIRCRAFT

The position of the aircraft after it had flown past the screen was determined accurately by an open shutter 35-mm movie camera developed for another project (ref 3). The camera was located about 250 ft from the center of the screens along the flight path. It was directed vertically upward with its lens at the same level as the induction plate. The film travelled immediately behind a transverse slit in the image plane in a direction opposite to that of the airplane.

The camera operated as a camera obscura. Each point on the airplane overhead was imaged on the film as it passed through the imaginary plane determined by the slit and the lens. An image point remained on the film as the film travelled backward with a speed of about 3 1/2 ft/sec while the airplane flew forward. The resulting photograph appears to be a distorted shadowgraph of the airplane (fig. C1).

The position and the velocity of an airplane can be computed from its photograph and the known geometry of the system by the use of similar triangles. Figure C2 indicates how this is accomplished. Since dimensions transverse to the flight path are not distorted by the motion,

$$\frac{h}{f} = \frac{a}{b} \tag{C1}$$

where h = unknown height of a photographed section of the airplane

f = focal length of the camera lens, 1.89 in. (0.1575 ft)

a = distance between two known transverse points on the airplane, obtained from dimension drawing of the airplane

b = measured distance between the two corresponding points on the photograph

For example, the diameter of the image of the engine housing of the B-26 on the film of figure C1 is 0.315 in. The actual diameter of the housing is 60 in. Hence,

$$h = (0.1575)\left(\frac{60}{0.315}\right) = 30 \text{ ft}$$

The height h is then corrected, again by means of the dimension drawings; to obtain the height of the belly of the airplane. The distance the airplane center is off the desired line of flight is easily determined by noting which part of the image lies in the center of the film. The heights and the displacements measured by this procedure are given in tables 1 and 2 in terms of the airplane wing span.

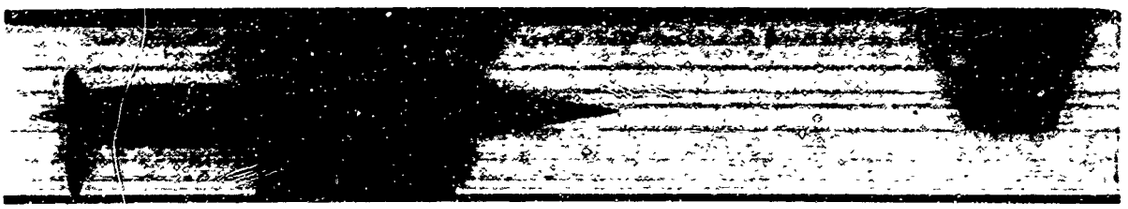

B—26

F—86

FIG. C1 PHOTOGRAPHS OF AIRPLANE OVERHEAD

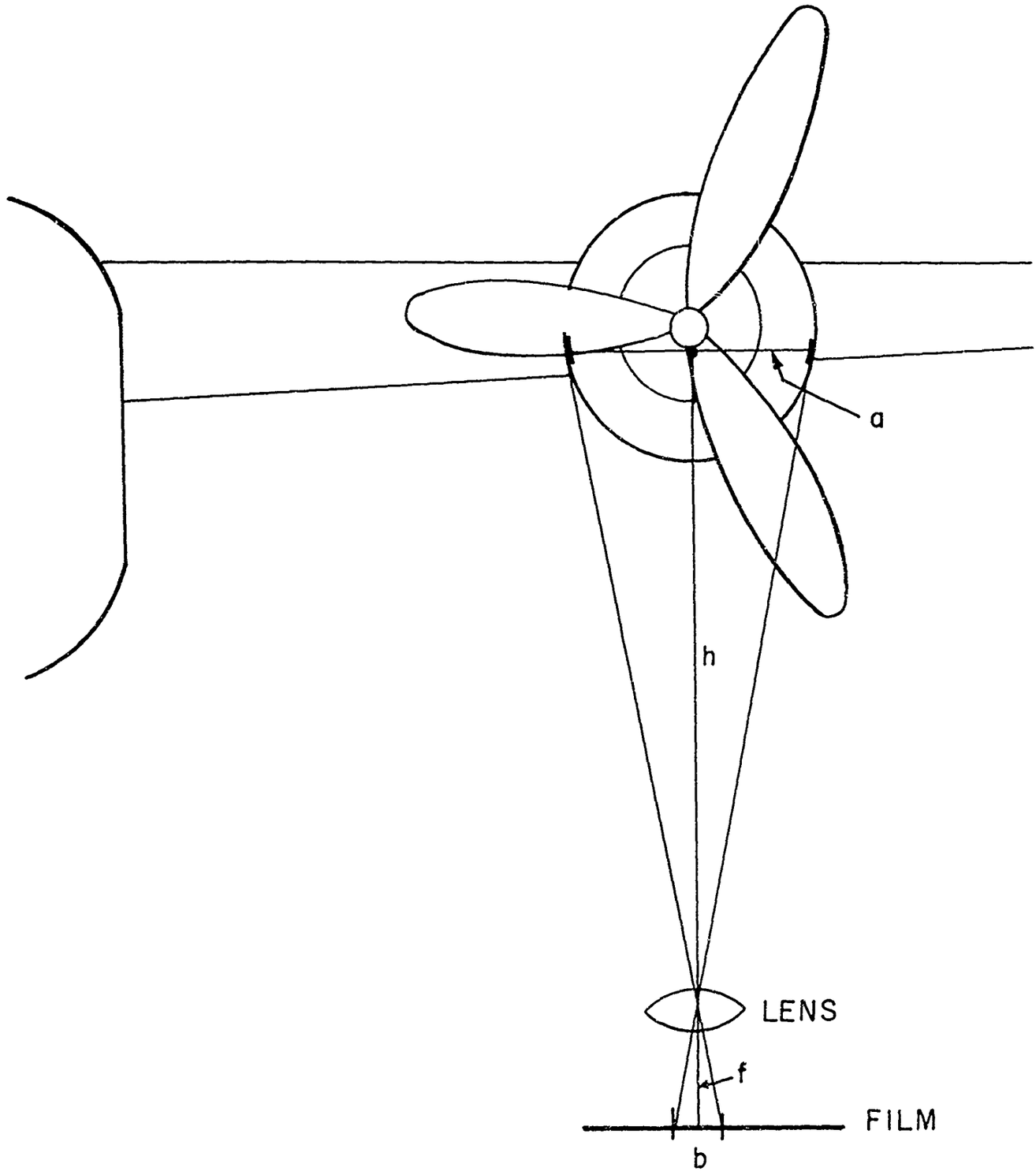

FIGURE C2 GEOMETRY OF THE OPTICAL SYSTEM

Once the height has been found from the transverse dimensions, the airplane velocity can be found from the longitudinal dimensions and the film velocity. This was not done in the present case inasmuch as the velocity was measured more directly with two photocells on the ground.

BLANK PAGE

DISTRIBUTION

Commanding General
U.S. Army Materiel Command
Washington, D. C., 20315
ATTN: AMCRD-SF, John R. Bird
ATTN: AMCRD-RS-PE-E

Commanding Officer
U. S. Army Electronics Research and Development Laboratory
Fort Monmouth, New Jersey
ATTN: Chief Scientist

Commander
Air Proving Ground Center
Eglin AFB, Florida
ATTN: PGGT, H. Maulshagen

Commander
Detachment 4, ASD
Eglin AFB, Florida
ATTN: ASQWW, E. T. Smith, 67-1449

Commanding Officer
Picatinny Arsenal
Ammunition Engineering Directorate
Dover, New Jersey
ATTN: Allan R. Nunes-Vais
ATTN: Albert L. Jamushevich
ATTN: MUCOM

Commanding General
Munitions Command
Dover, New Jersey
ATTN: John F. Lynch, AMC Project Manager for
Selected Ammunition

Commanding Officer
Frankford Arsenal
Philadelphia, Pa.
ATTN: J. W. Mitchell, SMUFA-1900

Headquarters
U.S. Army Combat Developments Command
Ft. Belvoir, Virginia
ATTN: Lt Col. T. Hess, Special Doctrine and Equipment Group

DISTRIBUTION (Cont'd)

Commanding General
Weapons Command
Rock Island, Illinois
ATTN: C. M. Erwin, AMSWE-RDW

Commander
U. S. Naval Ordnance Laboratory
Corona, California
ATTN: Charles Haber
ATTN: Documents Library

Department of the Navy
Bureau of Naval Weapons
Washington, D. C.
ATTN: R-12, E. S. Lamar
ATTN: RM-357, R. F. Gott
ATTN: RMMO-222, B. H. Tabb
ATTN: FWAA-541, F. L. Young
ATTN: RUUO, P. F. Fox
ATTN: DLI-3, Tech Library

Commander
Naval Research Laboratory
Washington, D. C.
ATTN: Wave Propagation Br
ATTN: Microwave Antennas & Components Br
ATTN: Technical Library

Commander
U. S. Naval Ordnance Lab
White Oak, Silver Spring, Maryland
ATTN: NA Div; E. A. White

Chief Operations Division
FS 400
Federal Aviation Agency
Washington, D. C. (4 copies)

Defense Documentation Center
Cameron Station Bldg No. 5
5010 Duke Street
Alexandria, Virginia
ATTN: DDCIR (20 copies)

INTERNAL DISTRIBUTION

Horton, B. M./Hochmuth, M. S., Lt. Col.
  Apstein, M./Gerwin, H. L./Guarino, P. A./Kalmus, H. P.
  Spates, J. E./Schwenk, C. C.
Hardin, C. D., Lab 100
Sommer, H., Lab 200
Hatcher, R. D., Lab 300
Hoff, R. S., Lab 400
Nilson, H., Lab 500
Flyer, I. N., Lab 600
Campagna, J. H./Apolenis, C. J., Div 700
DeMasi, R., Div 800
Landis, P. E., Lab 900
Seaton, J. W., 260
Krupen, Philip, 260 (5 copies)
Rogers, Elmer B., 844 (5 copies)
Landis, P. E., Lab 900
Technical Reports Unit, 800
Technical Information Office, 010 (5 copies)
HDL Library (5 copies)
Rotkin, I./Godfrey, T.B./Bryant, W. T.
Distad, M. F./McCoskey, R. E./Moorhead, J. G.
Bonnell, R., 040
Tremper, W., 843

AD_____ UNCLASSIFIED Accession No_____

Harry Diamond Laboratories, Washington, D. C. 20438

MEASUREMENT OF ELECTROSTATIC CHARGE ON AIRCRAFT - Philip Krupen, Elmer B. Rogers

TR-1267, 30 December 1964, 22 pp text, 10 illus, DA-1P010501A001 AMCMS Code: 5011.11.71200, HDL Proj. No. 36133, UNCLASSIFIED Report

The electrostatic charge on airplanes was determined from measurements of the charge induced on a large screen while the airplanes flew over it. The airplane charge was computed from a transfer function that involved the relaxation time of the sensing circuit and the passage time of the airplane. Corrections for variation in the height and displacement of the airplanes were made from laboratory measurements on scale models of the field equipment. The average charge on a jet-propelled F-86 fighter was found to be -35.4×10^{-8} coulomb and on a B-26 bomber, -0.56×10^{-8} coulomb. The corresponding aircraft potentials are approximately -141,000 and -1200 v.

Electrostatic charge

Aircraft charging

Charge measurement

AD_____ UNCLASSIFIED Accession No_____

Harry Diamond Laboratories, Washington, D. C. 20438

MEASUREMENT OF ELECTROSTATIC CHARGE ON AIRCRAFT - Philip Krupen, Elmer B. Rogers

TR-1267, 30 December 1964, 22 pp text, 10 illus, DA-1P010501A001 AMCMS Code: 5011.11.71200, HDL Proj. No. 36133, UNCLASSIFIED Report

The electrostatic charge on airplanes was determined from measurements of the charge induced on a large screen while the airplanes flew over it. The airplane charge was computed from a transfer function that involved the relaxation time of the sensing circuit and the passage time of the airplane. Corrections for variation in the height and displacement of the airplanes were made from laboratory measurements on scale models of the field equipment. The average charge on a jet-propelled F-86 fighter was found to be -35.4×10^{-8} coulomb and on a B-26 bomber, -0.56×10^{-8} coulomb. The corresponding aircraft potentials are approximately -141,000 and -1200 v.

Electrostatic charge

Aircraft charging

Charge measurement

AD_____ UNCLASSIFIED Accession No_____

Harry Diamond Laboratories, Washington, D. C. 20438

MEASUREMENT OF ELECTROSTATIC CHARGE ON AIRCRAFT - Philip Krupen, Elmer B. Rogers

TR-1267, 30 December 1964, 22 pp text, 10 illus, DA-1P010501A001 AMCMS Code: 5011.11.71200, HDL Proj. No. 36133, UNCLASSIFIED Report

The electrostatic charge on airplanes was determined from measurements of the charge induced on a large screen while the airplanes flew over it. The airplane charge was computed from a transfer function that involved the relaxation time of the sensing circuit and the passage time of the airplane. Corrections for variation in the height and displacement of the airplanes were made from laboratory measurements on scale models of the field equipment. The average charge on a jet-propelled F-86 fighter was found to be -35.4×10^{-8} coulomb and on a B-26 bomber, -0.56×10^{-8} coulomb. The corresponding aircraft potentials are approximately -141,000 and -1200 v.

Electrostatic charge

Aircraft charging

Charge measurement

AD_____ UNCLASSIFIED Accession No_____

Harry Diamond Laboratories, Washington, D. C. 20438

MEASUREMENT OF ELECTROSTATIC CHARGE ON AIRCRAFT - Philip Krupen, Elmer B. Rogers

TR-1267, 30 December 1964, 22 pp text, 10 illus, DA-1P010501A001 AMCMS Code: 5011.11.71200, HDL Proj. No. 36133, UNCLASSIFIED Report

The electrostatic charge on airplanes was determined from measurements of the charge induced on a large screen while the airplanes flew over it. The airplane charge was computed from a transfer function that involved the relaxation time of the sensing circuit and the passage time of the airplane. Corrections for variation in the height and displacement of the airplanes were made from laboratory measurements on scale models of the field equipment. The average charge on a jet-propelled F-86 fighter was found to be -35.4×10^{-8} coulomb and on a B-26 bomber, -0.56×10^{-8} coulomb. The corresponding aircraft potentials are approximately -141,000 and -1200 v.

Electrostatic charge

Aircraft charging

Charge measurement

REMOVAL OF EACH CARD WILL BE NOTED ON INSIDE BACK COVER, AND REMOVED CARDS WILL BE TREATED AS REQUIRED BY THEIR SECURITY CLASSIFICATION.